RSC Advances

PAPER

View Article Online
View Journal | View Issue

Cite this: *RSC Adv.*, 2017, **7**, 31093

Photocontrollable fluorogenic probes for visualising near-membrane copper(II) in live cells†

Buxiang Chen,[a] Liulin Wang,[a] Yanfei Zhao,[a] Yun Ni,[a] Chenqi Xin,[a] Chengwu Zhang,[a] Jinhua Liu,[a] Jingyan Ge,[b] Lin Li *[a] and Wei Huang*[ac]

In this work, we have described the design, synthesis, and characterisation of photocontrollable fluorogenic probe, **Mem-5**, which is equipped with a photolabile group (nitrobenzyl group), high brightness reporter (fluorescein), and membrane-anchoring unit (cholesterol or long aliphatic chain). This probe shows an intense fluorescence enhancement in response to copper(II) without interference from 45 other analytes, including metal cations, amino acids, and anions, under biological conditions (pH 6–9). The hydrolysis reaction is second-order, with $k = 9.01 \times 10^{-5}$ M^{-1} s^{-1}. The detection limit is 3.3×10^{-7} M in HEPES buffer (25 mM). The confocal fluorescence imaging results demonstrated that **Mem-5** can visualise near-membrane copper(II) in live mammalian cells. The clear advantage of our photocontrollable method is that it successfully avoids the influence of chemical species outside cells during near-membrane specific detection.

Received 27th March 2017
Accepted 31st May 2017

DOI: 10.1039/c7ra03559d

rsc.li/rsc-advances

Introduction

Cell plasma membranes are regarded as asymmetric due to their inner and outer leaflets having different compositions, based on the classic Singer–Nicolson model.[1] This prevents foreign substances from entering the cell barrier freely, ensuring a relatively stable environment within the cell,[2] but absorbs and digests material inside and outside by endocytosis, phagocytosis, or exocytosis.[3,4] Therefore, this lipid bilayer with embedded protein membranes is important for cell recognition, signal transduction, cellulose synthesis, microfibril assembly, and other mechanisms,[5] and can regulate cell life activities as turntables for crucial processes in neurobiology, muscle contraction, and cell signalling.[6,7] Given the pivotal role of cell plasma membranes, the development of membrane-specific fluorogenic probes to detect near-membrane elements has attracted increasing attention.[8–15]

Copper(II) content in the human body is the second most common trace element, and plays an essential role in human metabolism.[16] Copper(II) overload has been shown to cause a range of neurological diseases, such as Wilson's and Alzheimer's diseases.[17,18] High-affinity copper transporter 1 (Ctr1) drives the entry of copper(II) into cells,[19] while cells must eject excess copper(II) through the plasma membrane to maintain a low concentration of cytosolic free copper(II).[20] Effective methods for evaluating free copper(II) near or across the plasma membrane will aid understanding of the copper(II) transportation-related biological functions of cells. Regrettably, tools to precisely detect near-membrane copper(II) in live cells without interference by external copper(II) have still not been developed.

With this in mind, herein, we have successfully developed two new photocontrollable fluorogenic probes (Fig. 1) with different membrane anchors to image near-membrane copper(II) in live mammalian cells with good spatial and temporal controls using efficiently photolysis by ultraviolet (UV) light irradiation. **Mem-1/2** (structures shown in Fig. 2), which contain a cholesterol or 12-carbon aliphatic chain, served as membrane tracers, and their membrane staining ability was compared using this "piggyback" strategy.[21–23] As shown in Fig. 1, fluorescein hydrazide hydrolysed by copper(II) would normally be blocked due to the existence of a caged unit after membrane staining,[24] facilitating the complete accumulation of **Mem-5/6** with no fluorescence.[25] Subsequent UV irradiation will force removal of the caged group, releasing uncaged **Mem-3/4** (structures shown in Fig. 2),[26,27] which would then be hydrolysed by copper(II) to generate a specific localised and strong fluorescent signal.[28] Notably, the modularity of our probe design should enable this strategy to be readily applicable to the detection of other targets near the membrane.

[a]*Key Laboratory of Flexible Electronics (KLOFE), Institute of Advanced Materials (IAM), Jiangsu National Synergetic Innovation Center for Advanced Materials (SICAM), Nanjing Tech University (Nanjing Tech), 30 South Puzhu Road, Nanjing, 211816, P. R. China. E-mail: iamlli@njtech.edu.cn; iamwhuang@njtech.edu.cn*

[b]*Key Laboratory of Bioorganic Synthesis of Zhejiang Province, College of Biotechnology and Bioengineering, Zhejiang University of Technology, Hangzhou 310014, P. R. China*

[c]*Key Laboratory for Organic Electronics and Information Displays, Institute of Advanced Materials (IAM), Nanjing University of Posts & Telecommunications, 9 Wenyuan Road, Nanjing 210023, P. R. China*

† Electronic supplementary information (ESI) available: Synthesis and characterisation, photophysical spectra and background control images. See DOI: 10.1039/c7ra03559d

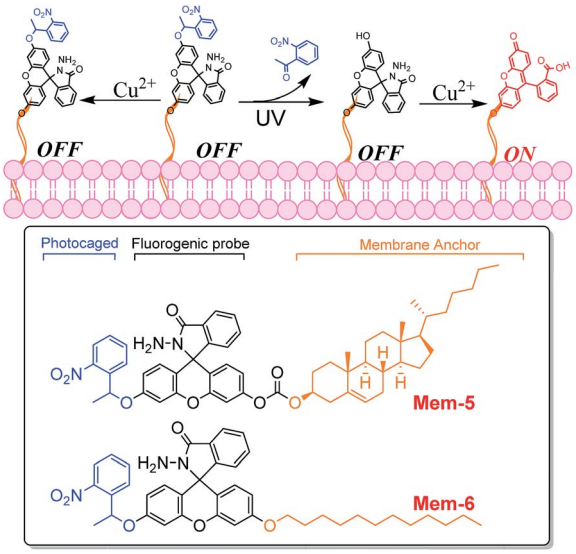

Fig. 1 Overall strategy of our photocontrollable fluorogenic probes, **Mem-5** and **Mem-6** (structures shown in box), for imaging membrane copper(II) in live cells.

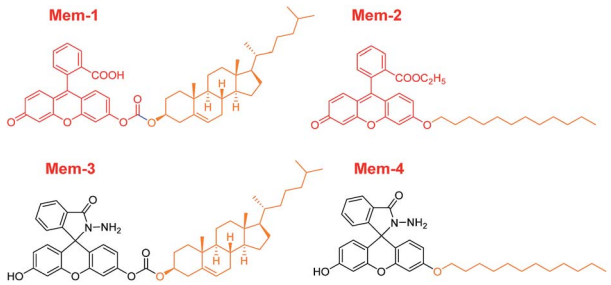

Fig. 2 Structures of membrane tracers, **Mem-1** and **Mem-2**, with different anchors, and unphotocontrollable fluorogenic probes, **Mem-3** and **Mem-4**, for imaging membrane copper(II) in live cells.

Experimental

Materials and instruments

All reagents and solvents were purchased from commercial suppliers and used without further purification, unless otherwise noted. *N*,*N*-Dimethylformamide (DMF) was distilled over CaH_2. Petroleum ether (PE, 60–90 °C), DCM, and ethyl acetate (EA) were used as eluents for flash column chromatography with Merck silica gel (0.040–0.063). 1-(1-Bromoethyl)-2-nitrobenzene was synthesised according to a literature procedure, while fluorescein and hydrazine hydrate were purchased from Adamas.[25] Cholesterol chloride and bromododecane were purchased from Tokyo Chemical Industry. Nuclear (Hoechst 33 342) and membrane (CM orange) trackers were purchased from Invitrogen. Human hepatocellular carcinoma (HepG2) cells and fetal bovine serum (FBS) were purchased from ATCC (HB-8065™) and Biological Industries (BI, 04-001-01ACS), respectively. Other reagents used in the experiments were purchased from Sigma-Aldrich and used without further purification unless otherwise noted. Distilled water was used throughout the experiments. Absorption spectra were recorded using SynergyHTX microplate reader or a Shimadzu UV-3600 UV-Vis-NIR spectrophotometer. Photoluminescence spectra were recorded using a HITACHI F4600 fluorescence spectrophotometer with excitation slit widths of 5 nm and emission slit widths of 10 nm. ^{1}H and ^{13}C NMR spectra were collected in $CDCl_3$ or DMSO-d^6 at 25 °C using an Avance AV-300 spectrometer. All photochemical reactions were conducted in an ultraviolet analyser ZF-20D. Ultrapure water was used to prepare all aqueous solutions. Fluorescein in 0.1 M NaOH ($\Phi = 0.85$) was used as the standard for quantum yield measurements. All spectroscopic measurements were performed in 25 mM HEPES buffer (pH 7.4) at 37 °C. All images were acquired in the same way at 20 °C on Zeiss LSM880 NLO (2 + 1 with BIG) confocal microscope system equipped with an objective LD C-Apochromat 63×/1.15 W Corr M27, 405 nm diode laser, argon ion laser (458, 488, and 514 nm), HeNe laser (543 and 594 nm), and 633 nm laser, with 8 AOTF channels for simultaneous control of 8 laser lines. A PMT detector ranging from 420 nm to 700 nm was used for steady-state fluorescence. Internal photomultiplier tubes were used to collect the signals in 8 bit unsigned 1024 × 1024 pixels at a scan speed of 200 Hz. Images were processed with Zeiss User PC Advanced for LSM system (BLUE).

Synthetic procedures

All reactions were carried out under a dry nitrogen atmosphere. Reaction progress was monitored by TLC on pre-coated silica plates (thickness, 250 μm) and spots were visualised using ceric ammonium molybdate, basic $KMnO_4$, UV light, or iodine.

Synthesis of Mem-5. In a 50 mL round bottom flask, triethylamine (0.014 mL) was added to a solution of nitrobenzyl-protected fluorescein hydrazide (50 mg, 0.10 mmol) in DMF (2 mL). The mixture was stirred for 5 min under a dry nitrogen atmosphere. Cholesteryl chloroformate (45.34 mg, 0.10 mmol) in chloroform (0.8 mL) was added dropwise to the solution. The reaction was stirred in an ice bath for another 8 h, followed by the addition of saturated ammonium chloride aqueous solution (10 mL) and extraction with ethyl acetate (3 × 30 mL). The organic layer was washed three times with brine, dried over anhydrous Na_2SO_4, and filtered. After removing solvent under reduced pressure, the residue was purified by flash column chromatography (silica gel, PE/EA = 1 : 1) affording the product as a pink solid (yield 60%). ^{1}H NMR (300 MHz, $CDCl_3$): δ (ppm) 8.03 (d, $J = 4.5$ Hz, 1H), 7.93 (t, $J = 4.5$ Hz, 1H), 7.75 (d, $J = 3$ Hz, 1H), 7.59 (t, $J = 7.5$ Hz, 1H), 7.45 (m, 3H), 7.09 (s, 1H) 7.02 (d, $J = 3$ Hz, 1H), 6.52 (m, 4H), 6.82 (dd, $J_1 = 4.5$ Hz, $J_2 = 1.5$, 1H), 6.65 (d, $J = 4.5$ Hz, 2H), 6.52 (d, $J = 3$ Hz, 2H), 6.05 (dd, $J_1 = 3$ Hz, $J_2 = 1.5$ Hz, 1H), 5.42 (s, 1H), 4.60 (dd, $J_1 = 6$ Hz, $J_2 = 3$ Hz, 1H) 3.52 (bs, NH_2), 2.48 (s, 2H), 2.00 (m, 5H), 1.56 (m, 10H), 1.33 (m, 4H), 0.91 (m, 22H), 0.68 (s, 3H). ^{13}C NMR (75 MHz, $CDCl_3$): δ (ppm) 166.41, 158.49, 152.49, 151.77, 150.66, 150.55, 139.16, 138.63, 134.26, 134.21, 133.05, 128.61, 128.43, 128.37, 128.30, 128.20, 127.50, 124.91, 123.94, 123.42, 123.37, 116.94, 116.51, 112.90, 112.66, 110.04, 103.36, 103.21, 79.31, 71.86, 56.80, 56.27, 50.11, 42.43, 39.83, 39.62, 37.98, 36.92, 36.65, 36.30, 35.87, 32.01,

31.96, 28.31, 28.09, 27.69, 24.38, 23.93, 23.67, 23.62, 22.90, 22.66, 21.16, 19.36, 18.83, 11.97.

Synthesis of Mem-6. To a stirred solution of nitrobenzyl-protected fluorescein hydrazide (50 mg, 0.10 mmol) in dry DMF (2 mL) was added Cs_2CO_3 (114.04 mg, 0.35 mmol) and bromododecane (25.16 mg, 0.10 mmol) under a dry nitrogen atmosphere. After being stirred for 8 h at 60 °C, the reaction was stopped with the addition of saturated aqueous ammonium chloride (10 mL). The mixture was extracted and isolated as described above in the procedure for **Mem-5**, to afford **Mem-6** as a pink solid (yield 62%). ^{1}H NMR (300 MHz, $CDCl_3$): δ (ppm) 8.04 (d, J = 4.5 Hz, 1H), 7.92 (t, J = 4.5 Hz, 1H), 7.74 (d, J = 4.5 Hz, 1H), 7.60 (t, J = 7.5 Hz, 1H), 7.46 (m, 3H), 7.01 (dd, J_1 = 3 Hz, J_2 = 1.5 Hz, 1H), 6.70 (d, J = 4.5 Hz, 1H), 6.52 (m, 4H), 6.04 (dd, J_1 = 3 Hz, J_2 = 1.5 Hz, 1H), 3.94 (t, J = 7.5 Hz, 2H), 3.63 (bs, NH_2), 1.70 (m, 4H), 1.42 (s, 1H), 1.26 (s, 19H), 0.87 (d, J = 7.5 Hz, 3H). ^{13}C NMR (75 MHz, $CDCl_3$): δ (ppm) 166.43, 160.40, 158.41, 153.23, 151.01, 138.79, 134.33, 134.27, 132.94, 129.83, 128.75, 128.60, 128.54, 128.11, 127.57, 124.94, 123.87, 135.35, 112.73, 112.47, 112.31, 110.20, 103.18, 103.00, 101.65, 71.85, 68.45, 63.17, 32.95, 32.02, 29.76, 29.73, 29.70, 29.67, 29.45, 29.22, 26.11, 23.68, 22.79, 14.21.

Photouncaging reactions

For *in vitro* analysis, different concentrations (2.0 μM for selectivity/kinetic experiments and 10.0 μM for pH titration experiments) of **Mem-5** were placed in quartz glassware and submitted to UV irradiation (500 μJ cm^{-2} at 400 nm) for 5 min at room temperature to generate uncaged **Mem-5** in HEPES buffer. In live cell imaging, cells were incubated with **Mem-5** (2.0 μM) for 20 min at 37 °C, followed by further UV irradiation (500 μJ cm^{-2}, 5 min) at room temperature in cover-free dishes to generate uncaged **Mem-5**.

Cell culture and cytotoxicity activity assay

HepG2 cells were cultured in Dulbecco's Modified Eagle's Medium (DMEM), containing 10% FBS, 100.0 mg L^{-1} streptomycin, and 100 IU mL^{-1} penicillin. HepG2 cells were seeded in glass-bottom dishes (Mattek) and grown to 70–80% confluency. The cytotoxicity activities of the probes were determined using an XTT colorimetric cell proliferation kit (Roche), following the manufacturer guidelines. Briefly, different cells were grown to 20–30% confluency (they would reach 80–90% confluency within 48–72 h in the absence of compounds) in 96-well plates under the conditions described above. The medium was aspirated, washed with PBS, and then treated, in duplicate, with 0.1 mL of the medium containing different concentrations of **Mem-1/2/3/4/5/6** (1–50 μM). Probes were applied from DMSO stocks, whereby DMSO never exceeded 1% in the final solution. The same volume of DMSO was used as a negative control, while the same volume of staurosporine (STS, 200 nM) was used as a positive control. After a total treatment time of 24 h, proliferation was assayed using the XTT colorimetric cell proliferation kit (Roche), following manufacturer guidelines (Fig. 4a).

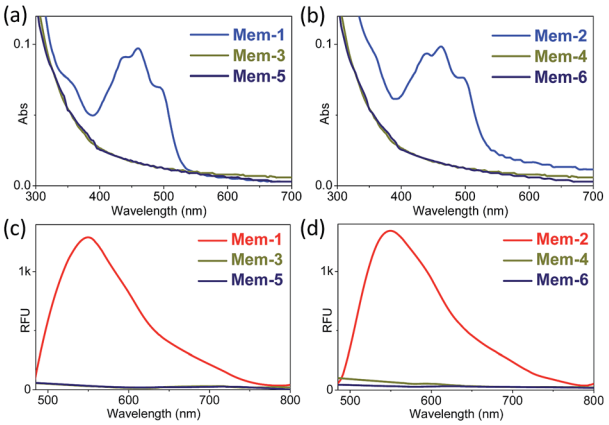

Fig. 3 Absorption spectra of (a) **Mem-1/3/5** and (b) **Mem-2/4/6**, and fluorescence emission spectra of (c) **Mem-1/3/5** and (d) **Mem-2/4/6** in HEPES buffer (probe concentration, 5.0 μM). Abs = absorbance, RFU = relative fluorescence units.

Live cells fluorescence imaging

For organelle-specific imaging experiments, the cells were incubated with **Mem-1** and **Mem-2** (1 μM prepared in fresh medium) for 20 min at 37 °C, followed by washing three times with PBS. To accurately visualise membrane copper, the cells were incubated with **Mem-3** and **Mem-5** (5 μM prepared in fresh medium) for 20 min at 37 °C. After washing three times with PBS, the selected cells were irradiated for 2 min with UV light through an ultraviolet analyser. The cells were then incubated with copper(II) (10 equiv.) for a further 60 min at 37 °C. Next, the cells were washed three times with PBS, then imaged with the Zeiss LSM880 NLO (2 + 1 with BIG) confocal microscope system (Fig. 2 and 3). Hoechst 33 342 (250 nM, E_x = 405 nm, PMT range = 420–460 nm) and CM orange (100 nM, E_x = 543 nm, PMT range = 550–650 nm) were used as nuclear and membrane trackers, respectively. Meanwhile, another identical set of samples was treated as described above, but without UV irradiation, as the negative control. Background signals of all images were verified to be nearly zero by imaging the same cells treated with a negative control.

Results and discussion

Synthesis and characterisation

To validate our design, two photocontrollable fluorogenic probes (**Mem-5/6**) and four additional control probes (**Mem-1/2/3/4**) were synthesised following modified literature methods,[29–31] as summarised in Scheme S1.† Two membrane tracers (**Mem-1/2**) with different membrane anchors were obtained from the condensation of fluorescein/fluorescein esters (reporter, a dye with high brightness) and cholesteryl chloroformate/bromododecane in ~50% yield. Fluorescein hydrazide, a copper(II)-responsive unit, was synthesised in one step with an overall yield of 92% from commercially available hydrazine hydrate and fluorescein, followed by coupling with membrane-targeting moieties to generate **Mem-3/4**, both in 50% yield. Nitrobenzyl-protected fluorescein hydrazide was

prepared by the condensation of fluorescein hydrazide and 1-(1-bromoethyl)-2-nitrobenzene in 54% yield in the presence of Cs_2CO_3. **Mem-5/6** (~60% yields) were prepared using a procedure similar to that described above for **Mem-3/4**. The compound structures were fully characterised by ^1H and ^{13}C NMR, with detailed synthetic procedures and original spectra described in the experimental section and ESI.†

To systemically demonstrate the potential utility of our newly developed probes as good fluorogenic systems for live cell imaging, we first evaluated their chemical, photophysical, and biological properties. As shown in Fig. 3a and b, under physiological conditions (HEPES buffer, pH 7.4), **Mem-1/2**, the membrane tracer references of **Mem-5/6**, had maximum absorptions at 460 nm, with two shoulder peaks at 440 and 460 nm, and an emission at 550 nm (Fig. 3c and d, $\Phi = \sim 0.15$ with fluorescein in 0.1 M NaOH as the reference). **Mem-1/2/3/4** showed nearly no absorption or emission ($\Phi = 0.001$–0.0015) at around the same wavelength, based on the closed-loop structure. A similar outcome was observed in organic solvent (ethanol, Fig. S1–S4†). Furthermore, two different membrane anchors had no effect on the photophysical properties of the probes, and the caged probes had very low fluorescence backgrounds or high S/N ratios for live cell imaging.

Subsequently, the cytotoxicity assays showed no obvious cell toxicity at concentrations up to 50 μM for **Mem-1/3/5** and 20 μM for **Mem-2/4/6**, in human hepatocellular carcinoma (HepG2) cells (Fig. 4a). The results showed that **Mem-1/3/5** with a cholesterol unit were more suitable for the living cell assay than the group a long aliphatic chain at high concentrations. Theoretically, a probe/plasma membrane lipid ratio must be lower than 1/100 for there to be no significant perturbation of the biomembrane properties in cell membrane staining.[32] Therefore, both **Mem-1/3/5** and **Mem-2/4/6** were suitable for living cell imaging at low working concentrations, because we incorporated a high brightness reporter in the probe design. Therefore, to establish that **Mem-1/2** was indeed a good membrane tracer for live cell imaging unequivocally, HepG2 cells were treated with **Mem-1/2**, followed by one-photon fluorescence imaging (background control shown in Fig. S5†). We observed fluorescent staining exclusively within the plasma membrane of the cells for **Mem-1** (Fig. 4b(2/3), 1 μM treatment for 20 min). Otherwise, **Mem-2**, the probe with a 12-carbon aliphatic chain, stained whole cells without specific localisation on the plasma membrane (Fig. 4b(7/8)). As shown in Fig. 4b(5), the green fluorescence signal of **Mem-1** overlapped well with the red fluorescence signal of the commercially available membrane tracker (CM-orange) with a high contrast ratio. Prolonged incubation of the cells with **Mem-1** did not lead to

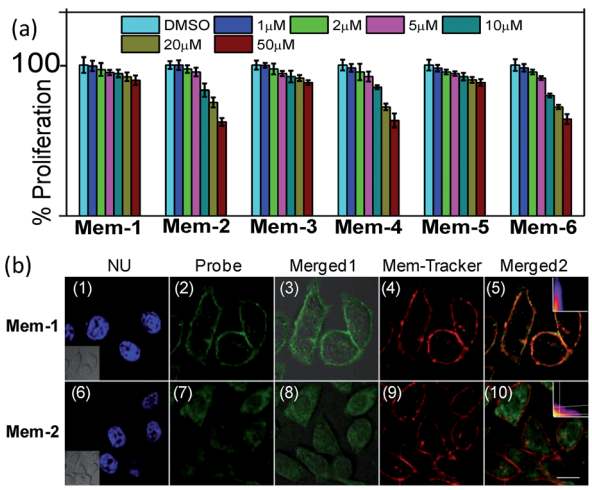

Fig. 4 (a) XTT assay profiles of **Mem-1/2/3/4/5/6**, error bars represent s.e.m. ($n = 3$). (b) One-photon fluorescence microscopy imaging of live HepG2 cells by control probes **Mem-1** and **Mem-2** (1 μM). Live cells were incubated with the probes for 20 min at 37 °C, followed by addition of a commercially available nuclear stain (NU, 250 nM) and membrane tracker (Mem-tracker, 100 nM), and then further incubation for 10 min before imaging. The excitation wavelength was 457 nm, while the PMT range was 500–550 nm for probes. Inset in (1) is the differential interference contrast image (DIC). (3) and (8) are merged images of (2) and (7) with related DIC, respectively; while (5) and (10) are merged images of (2)/(4) with the colocalisation analysis ($R = 0.80$) and (7)/(9) ($R = 0.04$), respectively. All images were acquired in the same way. Scale bar = 15 μm.

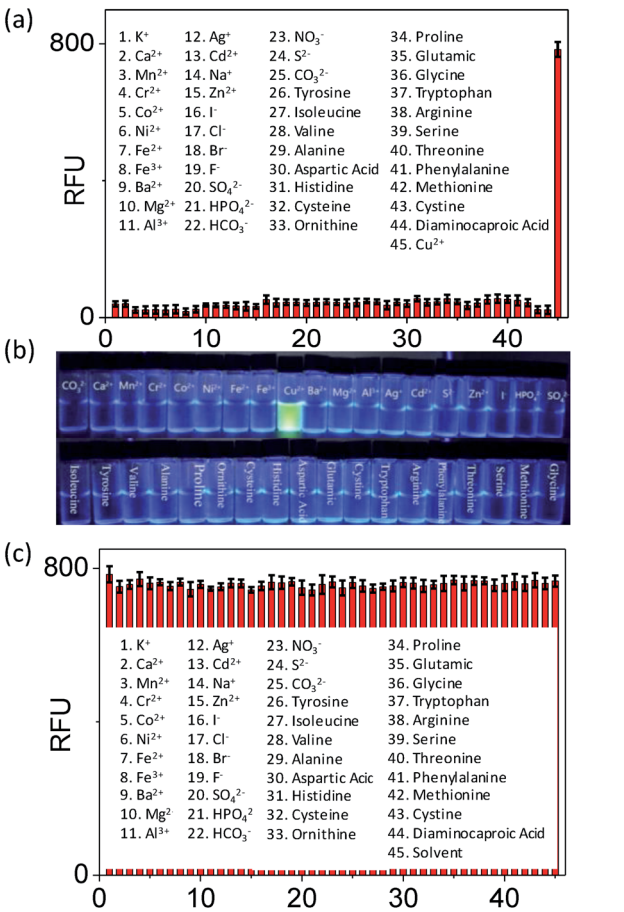

Fig. 5 (a) Effect of the 45 analytes (10 eq.) on uncaged **Mem-5** (2.0 μM, 5 min UV-illumination) in HEPES buffer. (b) Photo of fluorescence with the effect of analytes (10 eq.) on uncaged **Mem-5** (2.0 μM) in HEPES buffer after 60 min of incubation at 37 °C. (c) Effect of the analytes (50 eq.) on uncaged (5 min of UV radiation) **Mem-5** (2.0 μM) with Cu^{2+} (10 eq.) in HEPES buffer. Red bars represent the fluorescence intensity at 37 °C. Error bars represent s.e.m. ($n = 3$).

the staining of other lipid-like environments in intracellular organelles, indicating minimal probe internalisation, and confirming **Mem-1** as cell-membrane specific.

We next investigated whether **Mem-5** serves as an effective photocontrollable fluorogenic probe for visualising near-membrane copper(II) in live cells. Upon photolysis with UV irradiation (500 μJ cm^{-2} for 5 min), non-fluorescent **Mem-5** generated non-fluorescent uncaged **Mem-5**, according to a literature method.[24] To evaluate the selectivity of **Mem-5** toward copper(II) among a series of metal cations, amino acids and anions, 45 analytes (10 eq.), including K^+, Ca^{2+}, Mn^{2+}, Cr^{2+}, Co^{2+}, Ni^{2+}, Fe^{2+}, Fe^{3+}, Ba^{2+}, Mg^{2+}, Al^{3+}, Ag^+, Cd^{2+}, Na^+, Cu^{2+}, tyrosine, 2,6-diaminocaproic acid, isoleucine, valine, alanine, aspartic acid, histidine, cysteine, ornithine, proline, glutamic acid, glycine, tryptophan, arginine, serine, threonine, phenylalanine, methionine, cystine, CO_3^{2-}, I^-, Cl^-, Br^-, F^-, SO_4^{2-}, HPO_4^{2-}, HCO_3^-, S^{2-}, and NO_3^-, were incubated with uncaged **Mem-5** in HEPES buffer at 37 °C for 1 h, as shown in Fig. 5. A significant fluorescence enhancement in **Mem-5** was observed when copper(II) was added only, while other species had a negligible fluorescent intensity (Fig. 5a) with little interference (Fig. 5c). These results illustrate that **Mem-5** had a high selectivity for copper(II) recognition.

As the pH of the cell cytosol is between 6.8 and 7.4,[33] we attempted to determine whether the probe could emit fluorescence and be stable under these conditions. Therefore, the effect of pH on the fluorescence response of **Mem-5** to copper(II) was tested in a pH titration experiment. **Mem-5** was found to be stable in a wide pH range of 5–9, and showed a better response to copper(II) in the region pH 6–9 (Fig. 6a) after photolysis. When copper(II) (10 equiv.) was added to uncaged **Mem-5** (2 μM) in HEPES buffer, the fluorescence intensity increased gradually with time (Fig. 6b). The ^{1}H-NMR titration experiments of **Mem-3** with different equivalents of copper(II) indicated that fluorescein hydrazide was hydrolysed by copper(II) under these conditions (Fig. S6†). Next, the introduction of an increasing copper(II) concentration into the solution of uncaged **Mem-5** (2 μM) induced a gradual increase in the emission at around 525 nm (Fig. 6c). The slopes of the plots had a pseudo-first-order rate constant. A plot of the rate constants *vs.* copper(II) concentrations was a straight line passing through the origin, indicating that the reaction is second-order overall, with $k = 9.01 \times 10^{-5}$ M^{-1} s^{-1} (Fig. 6d).[34] Fluorescence intensities also exhibited a linear relationship with the copper(II) concentration, as shown in Fig. S7† ($R^2 = 0.97$). A linear regression curve was fitted to these normalised fluorescent intensity data, and the

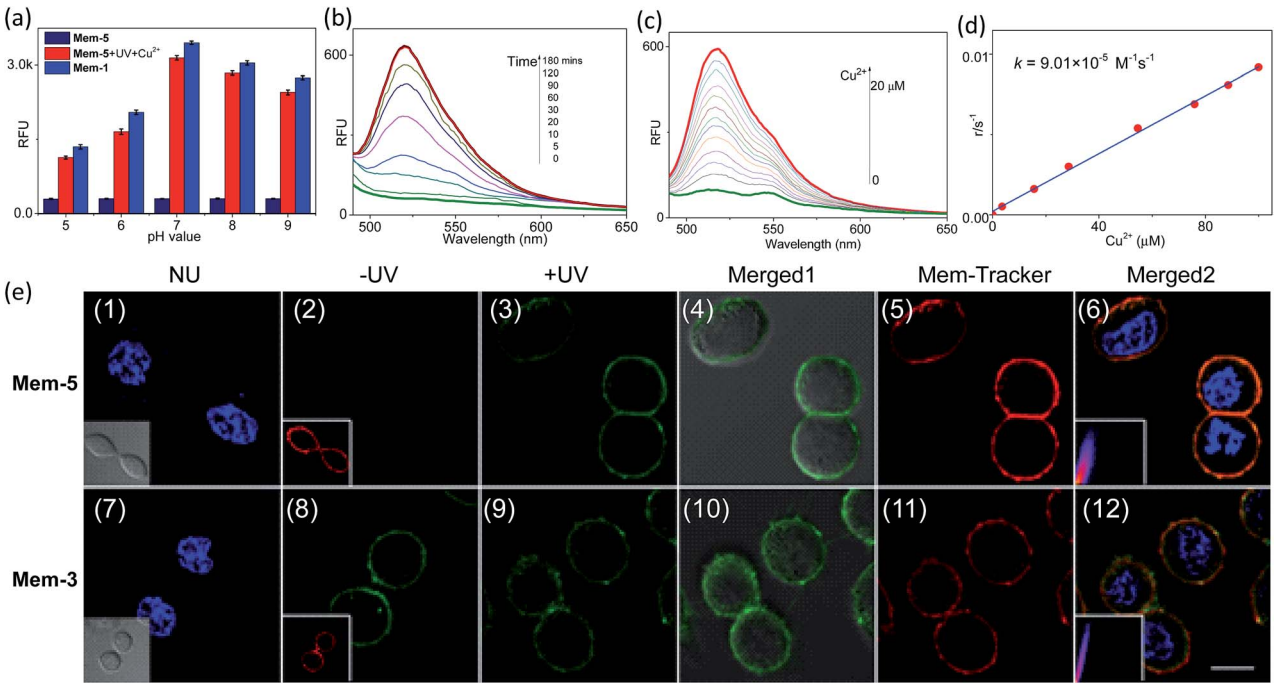

Fig. 6 (a) Fluorescence intensities (E_x = 455 nm) at 525 nm of **Mem-1/5** (10 μM) and uncaged **Mem-5** (10 μM)/Cu^{2+}(10 equiv.) at various pH values based on pH titration, error bars represent s.e.m. (n = 3). (b) Fluorescence spectra of uncaged **Mem-5** (2 μM) in the presence of Cu^{2+} (10 equiv.) for various periods (0–180 min). (c) Fluorescence intensities of uncaged **Mem-5** (2 μM) in the presence of increasing Cu^{2+} concentration (0–10 equiv.) (d) Plot of rate constants *vs.* Cu^{2+} concentrations. Reaction buffer was 25 mM HEPES (pH = 7.4), and the reaction temperature was 37 °C. (e) One-photon fluorescence microscopy imaging of live HepG2 cells by control probe **Mem-3/5** (2 μM). Live cells were incubated with the probe for 20 min at 37 °C, followed by UV(+) or UV(−) irradiation (5 min) at room temperature and addition of Cu^{2+} (10 equiv.) for another 20 min at 37 °C. The cells were then incubated with commercially available nuclear stain (NU, 250 nM) and membrane tracker (Mem-tracker, 100 nM), then further incubated for 10 min at 37 °C before imaging. The excitation wavelength and PMT range were 488 and 500–550 for both probes. Insets in (1)/(7) are the differential interference contrast images (DIC), while those in (2)/(8) are related mem-tracker channel images. (4) and (10) are merged images of (3) and (9) with related DIC, respectively, while (6) and (12) are merged images of (3)/(5)/related nuclear stain with the inset of colocalization analysis of (3)/(5) (R = 0.85) and (9)/(11)/related nuclear stain with the inset of colocalization analysis of (9)/(11) (R = 0.87), respectively. All images were acquired in the same way. Scale bar = 15 μm.

point at which the regression line crossed the axis was considered the detection limit (3.3×10^{-7} M).

Finally, encouraged by these results, we determined whether **Mem-5** worked as a specific probe for imaging near-membrane copper(II). As shown in Fig. 6e, HepG2 cells were incubated with **Mem-3/5** in the presence of copper(II). Cells treated with **Mem-5** without UV irradiation showed no fluorescence, indicating temporal control of the "caging" strategy (Fig. 6e(2)). However, significant fluorescent enhancement of **Mem-3**-treated cells was observed using the same procedure (Fig. 6e(8)). Upon UV irradiation, a gradual increase in green fluorescence was observed both in **Mem-5** (Fig. 6e(3)) and **Mem-3**-treated cells (Fig. 6e(9)). The same cells were simultaneously treated with commercially available Mem-tracker to independently verify the localisation results. Both **Mem-5** and **Mem-3**-treated cells showed similar membrane-specific images by comparing the colocalisation analysis in Fig. 6e(6) and (12), indicating the strategy was amenable to the original design principle. Therefore, our photocontrollable method was successfully used to qualitatively detect near-membrane copper(II).

Conclusions

In this work, we have described the designed photocontrollable fluorogenic probe, **Mem-5**, which can visualise near-membrane copper(II) *via* fluorescence imaging, and is equipped with a photolabile group, high brightness reporter, and membrane-anchoring unit (cholesterol or long aliphatic chain). This probe shows an intense fluorescence enhancement in response to copper(II) without interference from 45 other analytes, including metal cations, amino acids and anions, under biological conditions. Live-cell imaging results indicate that the probe can detect near-membrane copper(II) after membrane anchoring using a photo-labile spatial and temporal control releasing method. The probe could be very useful for monitoring the homeostasis of near-membrane copper(II). A clear advantage of our photocontrollable method is that it successfully avoids the influence of chemical species outside cells during near-membrane specific detection. An important unresolved issue from this study is the lack of sensitivity for recording copper(II) across the membrane.

Acknowledgements

This work was financially supported by the National Natural Science Foundation of China (81672508, 61505076), Natural Science Foundation of Jiangsu Province (BK20140951), Natural Science Foundation of Zhejiang Province (LQ16B020003), and Key University Science Research Project of Jiangsu Province (Grant 16KJA180004).

Notes and references

1 S. J. Singer and G. I. Nicolson, *Science*, 1972, **175**, 720–731.
2 H. Lodish, A. Berk, S. L. Zipursky, P. Matsudaira, D. Baltimore and J. Darnell, *Molecular Cell Biology*, Scientific American Books, New York, 4th edn, 2004.
3 L. Wu, E. Hamid, W. Shin and H. Chiang, *Annu. Rev. Physiol.*, 2014, **76**, 301–331.
4 G. Meer, D. R. Voelker and G. W. Feigenson, *Nat. Rev. Mol. Cell Biol.*, 2008, **9**, 112–124.
5 Z. Darwich, A. S. Klymchenko, D. Dujardin and Y. Mély, *RSC Adv.*, 2014, **4**, 8481–8488.
6 D. Lingwood and K. Simons, *Science*, 2010, **327**, 46–50.
7 E. Sezgin, I. Levental, S. Mayor and C. Eggeling, *Nat. Rev. Mol. Cell Biol.*, 2017, **18**, 361–374.
8 J. L. Pincus, C. Y. Jin, W. J. Huang, H. K. Jacobs, A. S. Gopalan, Y. J. Song, J. A. Shelnutta and D. Y. Sasaki, *J. Mater. Chem.*, 2005, **15**, 2938–2945.
9 L. Li, X. Q. Shen, Q.-H. Xu and S. Q. Yao, *Angew. Chem., Int. Ed.*, 2013, **52**, 424–428.
10 Y. Xia and L. Peng, *Chem. Rev.*, 2013, **113**, 7880–7929.
11 Z. Liu, T. P. Yang, X. Li, T. Peng, H. C. Hang and X. D. Li, *Angew. Chem., Int. Ed.*, 2015, **54**, 1149–1152.
12 T. Peng and H. C. Hang, *J. Am. Chem. Soc.*, 2015, **137**, 556–559.
13 M. D. Molin, Q. Verolet, A. Colom, R. Letrun, E. Derivery, M. Gonzalez-Gaitan, E. Vauthey, A. Roux, N. Sakai and S. Matile, *J. Am. Chem. Soc.*, 2015, **137**, 568–571.
14 I. A. Karpenko, M. Collot, L. Richert, C. Valencia, P. Villa, Y. Mély, M. Hibert, D. Bonnet and A. S. Klymchenko, *J. Am. Chem. Soc.*, 2015, **137**, 405–412.
15 R. J. Radford, W. Chyan and S. J. Lippard, *Chem. Sci.*, 2013, **4**, 3080–3084.
16 D. Strausak, J. F. B. Mercer, H. H. Dieter, W. Stremmel and G. Multhaup, *Brain Res. Bull.*, 2001, **55**, 175–185.
17 A. Robert, Y. Liu, M. Nguyen and B. Meunier, *Acc. Chem. Res.*, 2015, **48**, 1332–1339.
18 O. Bandmann, K. H. Weiss and S. G. Kaler, *Lancet Neurol.*, 2015, **14**, 103–113.
19 B. E. Kim, T. Nevitt and D. J. Thiele, *Nat. Chem. Biol.*, 2008, **4**, 176–185.
20 B. J. McCranor, H. Szmacinski, H. H. Zeng, A. K. Stoddard, T. Hurst, C. A. Fierke, J. R. Lakowicz and R. B. Thompson, *Metallomics*, 2014, **6**, 1034–1042.
21 M. R. Krause and S. L. Regen, *Acc. Chem. Res.*, 2014, **47**, 3512–3521.
22 E. Ikonen, *Nat. Rev. Mol. Cell Biol.*, 2008, **9**, 125–138.
23 C. S. Lim, M. Y. Kang, J. H. Han, I. A. Danish and B. R. Cho, *Chem.–Asian J.*, 2011, **6**, 2028–2033.
24 L. Li, J. Y. Ge, H. Wu, Q.-H. Xu and S. Q. Yao, *J. Am. Chem. Soc.*, 2012, **134**, 12153–12160.
25 L. Yuan, W. Y. Lin, Z. M. Cao, L. L. Long and J. Z. Song, *Chem.–Eur. J.*, 2011, **17**, 689–696.
26 Y. R. Zhao, Q. Zheng, K. Dakin, K. Xu, M. L. Martinez and W. H. Li, *J. Am. Chem. Soc.*, 2004, **126**, 4653–4663.
27 I. Aparici-Espert, M. C. Cuquerella, C. Paris, V. Lhiaubet-Vallet and M. A. Miranda, *Chem. Commun.*, 2016, **52**, 14215–14218.
28 C. Wu, Q. N. Bian, B.-G. Zhang, X. Cai, S.-D. Zhang, H. Zheng, S.-Y. Yang and Y.-B. Jiang, *Org. Lett.*, 2012, **14**, 4198–4201.
29 V. Dujols, F. Ford and A. W. Czarnik, *J. Am. Chem. Soc.*, 1997, **119**, 7386–7387.

30 R. L. Zhang, J. Zhao, G. M. Han, Z. J. Liu, C. Liu, C. Zhang, B. H. Liu, C. L. Jiang, R. Y. Liu, T. T. Zhao, M. Y. Han and Z. P. Zhang, *J. Am. Chem. Soc.*, 2016, **138**, 3769–3778.
31 J. F. Hulvat, M. Sofos, K. Tajima and S. I. Stupp, *J. Am. Chem. Soc.*, 2005, **127**, 366–372.
32 M. Collot, R. Kreder, A. L. Tatarets, L. D. Patsenker, Y. Melya and A. S. Klymchenko, *Chem. Commun.*, 2015, **51**, 17136–17139.
33 J. Llopis, J. Michael McCaffery, A. Miyawaki, M. G. Farquhar and R. Y. Tsien, *Proc. Natl. Acad. Sci. U. S. A.*, 1998, **95**, 6803–6808.
34 J. H. Lee, C. S. Lim, Y. S. Tian, J. H. Han and B. R. Cho, *J. Am. Chem. Soc.*, 2010, **132**, 1216–1217.